XXI ICTAM, 15–21 August 2004, Warsaw, Poland

POLOIDAL-TOROIDAL DECOMPOSITION IN CYLINDRICAL VON KÁRMÁN FLOW

Piotr Boronski, Laurette Tuckerman
LIMSI (CNRS-UPR 3251), Department of Mechanics, BP 133 91403 Orsay, France

Summary The goal of the VKS experiment is to observe a laboratory-scale *dynamo effect* in the cylindrical von Kármán flow. Because there exists at present no complete numerical treatment of this configuration, we have developed an efficient three-dimensional pseudo-spectral code capable of solving the Navier-Stokes equations in a finite cylindrical geometry, to be coupled with the Maxwell equations. A *poloidal-toroidal* decomposition insures that fields are divergence-free by construction which is very important for applications to the magnetohydrodynamic case. The cylindrical domain is treated by using in the radial direction a polynomial basis which is regular at the domain axis. The satisfaction of high-order and/or coupled boundary conditions is guaranteed by the *influence matrix* method.

MOTIVATION

The *dynamo effect* is thought to be responsable for planetary and solar magnetic field. The VKS (von Kármán Sodium) experiment [1] aims to reproduce this effect at laboratory scales. Our goal is to develop a fully three-dimensional magnetohydrodynamic code capable of numerically simulating this experiment. Two features make this a particularly challenging task: a cylindrical geometry is used in conformity with the experiment, and the velocity and magnetic fields are constructed so as to be exactly divergence-free. Although three-dimensional coupled magnetohydrodynamic codes have been written in spherical geometries, to our knowledge, there exist no such codes in a cylindrical geometry of finite height.
A secondary motivation is to study the advantages and drawbacks of a pseudo-spectral method based on potentials of the velocity and magnetic fields, as well as to understand the importance of the regularity condition at the axis in a cylindrical geometry.

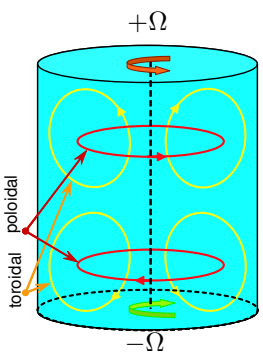

Figure 1. The simulated configuration. The counter-rotating discs generate two main flow structures - *toroidal* and *poloidal*.

MAIN ASSUMPTIONS

The configuration simulated consists of a conducting fluid enclosed in a cylinder of radius R and height h whose upper and bottom bases rotate in opposite directions with angular velocity Ω (fig. 1), generating the von Kármán swirling flow. This flow is considered to be a good candidate for a self-sustained dynamo [1]. The system is described by the Navier-Stokes and Maxwell equations coupled by induction and the magnetic tension and pressure.

$$\partial_t \mathbf{u} + (\mathbf{u}\cdot\boldsymbol{\nabla})\,\mathbf{u} + \tfrac{1}{\rho\mu}(\mathbf{B}\cdot\boldsymbol{\nabla})\,\mathbf{B} = -\tfrac{1}{\rho}\boldsymbol{\nabla}\left(p + \tfrac{1}{2\mu}B^2\right) + \nu\nabla^2\mathbf{u} \quad (1a)$$

$$\partial_t \mathbf{B} = \boldsymbol{\nabla}\times(\mathbf{u}\times\mathbf{B}) + \tfrac{1}{\rho\mu}\nabla^2\mathbf{B} \quad (1b)$$

$$\boldsymbol{\nabla}\cdot\mathbf{u} = \boldsymbol{\nabla}\cdot\mathbf{B} = 0 \quad (1c)$$

where $\mathbf{u}$ and $\mathbf{B}$ are the velocity and magnetic fields. No-slip boundary conditions are imposed on $\mathbf{u}$ while continuity with a surrounding insulating region is to be imosed on $\mathbf{B}$. Both the velocity $\mathbf{u}$ and the magnetic field $\mathbf{B}$ are required to be solenoidal; for $\mathbf{B}$ this is especially crucial [2]. For this reason, we represent $\mathbf{u}$ and $\mathbf{B}$ by the *poloidal-toroidal* decomposition given by:

$$\mathbf{u}(r,\theta,z) = \boldsymbol{\nabla}\times(\psi\hat{\mathbf{e}}_\mathbf{z}) + \boldsymbol{\nabla}\times\boldsymbol{\nabla}\times(\varphi\hat{\mathbf{e}}_\mathbf{z}) \quad (2)$$

where ψ and φ are scalar potentials. To simplify the description, we consider only the hydrodynamic equations (1a); the numerical scheme is applied in an analogous way to the magnetic part (1b). Substituting (2) for the velocity field $\mathbf{u}$ in (1a), we derive equations for ψ and φ by taking the $\hat{\mathbf{e}}_\mathbf{z}$ component of the curl and double curl of (1a), resulting in:

$$(\partial_t - \nu\Delta)\,\Delta_h\psi = \hat{\mathbf{e}}_\mathbf{z}\cdot(\boldsymbol{\nabla}\times\mathbf{b}) \quad (3a)$$

$$(\partial_t - \nu\Delta)\,\Delta\Delta_h\varphi = \hat{\mathbf{e}}_\mathbf{z}\cdot(\boldsymbol{\nabla}\times\boldsymbol{\nabla}\times\mathbf{b}) \quad (3b)$$

where $\mathbf{b}$ contains all nonlinear terms resulting from (1a). As for boundary conditions, the potentials ψ and φ cannot be completely decoupled and in the no-slip case give:

$$u_r:\ \tfrac{1}{r}\partial_\theta\psi + \partial^2_{rz}\varphi = 0 \qquad \begin{cases} r=R \\ z=\pm h \end{cases} \quad (4a)$$

$$u_\theta:\ \partial_r\psi - \tfrac{1}{r}\partial^2_{\theta z}\varphi = \begin{cases} 0 & r=R \\ \pm r\Omega(r) & z=\pm h \end{cases} \quad (4b)$$

$$u_z:\ \Delta_h\varphi = 0 \qquad r=R \quad (4c)$$

Additional conditions must be imposed on the sixth-order PDE system (3). Some of these are gauge conditions, whose purpose is to select among the potentials ψ and φ which yield the same $\mathbf{u}$. Others are due to the necessity to make the

differentiation leading to (3) reversible; these generalized integration constants insure that (3) leads to the same solution as (1a). The general form of these conditions was given in [3] and in our case gives

$$\varphi = 0 \qquad z=\pm h \tag{5a}$$

$$r\partial_{rz}\Delta_h\psi - \partial_\theta\Delta\Delta_h\varphi = 0 \qquad r=R \tag{5b}$$

NUMERICAL APPROACH

Axis condition

In a cylindrical geometry, the *axis condition* expresses the requirement that functions be continuous and infinitely differentiable at the axis. If a Fourier representation is used in the angular direction, this condition links the Fourier mode number with the degree and parity of the polynomial used in the radial direction (6) (as in the case of cylindrical Bessel functions):

$$f(r,\theta,z) = \sum_{\substack{k=0\ldots K \\ m=-M\ldots M \\ n=|m|\ldots N\,(m+n\ even)}} f^*_{m,n,k}\, e^{im\theta} r^n z^k \tag{6}$$

We choose a orthogonal basis of radial polynomials [4] satisfying the regularity condition at the cylinder axis. The polynomials are solutions of a Sturm-Liouville equation and are related to the shifted Jacobi polynomials. Taking into account the symmetry and degree relation significantly reduces the numerical cost of the algorithm, and more importantly, enforces the correct balance between the representable radial and azimuthal variation of the flow near the axis. This uniform scaling is achieved because, for each Fourier mode number, the associated radial polynomials decay sufficiently fast at the origin (fig. 2). The difference between a regularized and a non-regularized treatment is schematically demonstrated on figure 3.

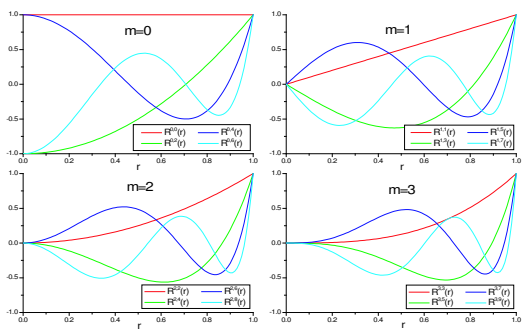

Figure 2. The radial polynomials [4]. The first four polynomials for the different Fourier modes $m = 0 \ldots 3$ have been plotted. The polynomials associated with Fourier wave number m contain powers $m, m+2, \ldots, N$ of r.

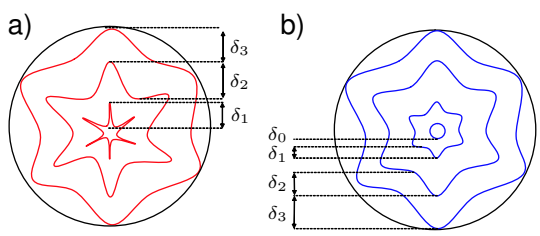

Figure 3. The visual interpretation of a pole singularity. The wavy lines represents schematically the profile of $e^{im\theta}P(r)$. a) A singular case: $P(r) \approx O(1)$; $\delta_1 \approx \delta_2 \approx \delta_3$. The peaks near to the origin are much steeper than those near the boundary. b) A regularized case: $P(r) = O(r^m)$ (here $m \geq 6$) ; $\delta_0 < \delta_1 < \delta_2 < \delta_3$. The peaks near the origin are of similar steepness to those near to the boundary.

Imposing the boundary condition

In order to satisfy the more complicated or coupled boundary conditions, we use the influence matrix technique. The main idea is to decompose the solution into particular and homogenous contributions. Simple decoupled boundary conditions are substituted for the actual conditions (4, 5) at each of these steps. The influence matrix measures the "influence" of each of the simplified boundary conditions on the quantities (4, 5) which are required to be zero for the final solution. Once the particular solution is calculated, the influence matrix is inverted to determine the coefficients of the Greens functions whose superposition is the required homogeneous contribution.

References

[1] Bourgoin M., Marié L., Pétrélis F., Gasquet C., Guigon A., Luciani J.B., Moulin M., Namer F., Burguete J., Chiffaudel A., Dauvid F., Fauve S., Odier P., Pinton J.F., MHD measurements in the von Kármán sodium experment, *Phys. Fluids*, **14**, 9 2002

[2] Brackbill J.U., Barnes D.C., The Effect of Nonzero $\nabla\cdot\mathbf{B}$ on the Numerical Solution of the Magnetohydrodynamic Equations, *J. Comput. Phys.* **35** 1980

[3] Marqués F., On boundary conditions for velocity potentials in confined flows: Application to Couette flow *Phys. Fluids A*, **2** 1990.

[4] Matsushima T. & Marcus P.S., A Spectral Method for Polar Coordinates, *J. Comput. Phys.* **120**, 365 (1995)